ELSEVIER

Ceramics International 33 (2007) 511–514

CERAMICS INTERNATIONAL

www.elsevier.com/locate/ceramint

Luminescence properties of Eu-doped SnO_2

Sung-Sik Chang [a,*], M.S. Jo [b]

[a] Department of Ceramic Engineering, Kangnung National University, Kangwondo 210-702, South Korea
[b] Department of Electrical Engineering, Kangnung National University, Kangwondo 210-702, South Korea

Received 18 July 2005; received in revised form 12 September 2005; accepted 12 October 2005
Available online 25 January 2006

Abstract

SnO_2 samples were sintered with an addition of Eu_2O_3 in nitrogen ambience by means of conventionally mixed oxides (CMO). The effects of Eu's addition on the luminescence properties are studied by photoluminescence (PL) at room temperature and low temperature, as well as photoluminescence excitation (PLE) spectroscopy. Structural properties are further studied by X-ray diffraction (XRD) and Raman spectroscopy. The addition of Eu results in efficient sharp luminescence peaks at 590 nm associated with d to f transition. The excitation energy higher than 3.6 eV yields an efficient energy transfer.

Keywords: A. Powders; B. Spectroscopy; C. Optical properties

1. Introduction

Tin oxide (SnO_2), an n-type semiconductor with a wide band gap (E_g = 3.6 eV at 300 K), is extensively used as a functional material for optoelectronic devices [1], conductive electrodes and transparent coatings due to its good conductivity and transparency in the visible spectrum [2,3], solar cells [4,5], and catalyst support [6]. The variation of grain size, the concentration of oxygen vacancies and electrical properties of tin oxide as bulk as well as forms of thin films are also widely studied. A large number of research works have been focused on the electrical properties of SnO_2, especially for sensor and catalyst. Whereas, only a small amount of work is devoted to the luminescence properties of SnO_2, namely SnO_2-based phosphors. The reported luminescence bands from SnO_2 are around 2.4–2.5 and 2.9–3.1 eV [7–9]. The origins of these luminescence bands are not clearly understood. In general, oxygen vacancies, which usually act as radiative centers, play an important role in the luminescence properties of the metal oxide semiconductors.

Rare-earth europium oxide has been potentially useful and studied extensively for various optical and electronic properties such as optical waveguide, optical filter, and capacitors [10–12]. Further, rare-earth-doped luminescent materials, namely phosphors, are widely applied for emissive displays and fluorescent lamps. Phosphors are mostly composed of solid inorganic materials consisting of a host lattice with intentional doping of impurities. The properties of luminescence depend on the host material. Rare-earth added inorganic materials exhibit several sharp emission lines in the visible spectral range. Further, rare-earth-doped semiconductors have been studied extensively for optoelectronic devices. This paper reports the feasibility of SnO_2-based phosphors. The luminescence properties of SnO_2-based phosphors are investigated by photoluminescence (PL) spectroscopy at room temperature and low temperature. The photoluminescence excitation (PLE) spectra are obtained to investigate the energy transfer between host SnO_2 and added Eu_2O_3. Further, the structural properties are examined by X-ray diffractometry (XRD) and Raman spectroscopy.

2. Experimental

The inorganic reagents are SnO_2 and Eu_2O_3. The initial composition is $(1-x)\ SnO_2{\cdot}xEu_2O_3$, where x varies 0 to 0.04. The pertinent composition is weighed and ball milled in ethanol for 24 h, dried, and pressed into pellets 5 mm in diameter and 1 mm thick. The samples are sintered at 1350 °C for 2 h in N_2 ambience of a tube furnace and cooled down in N_2 ambience.

* Corresponding author. Tel.: +82 33 640 2366; fax: +82 33 640 2244.
E-mail address: chang@knusun.kangnung.ac.kr (S.-S. Chang).

0272-8842/$32.00
doi:10.1016/j.ceramint.2005.10.021

The PL equipment consists of a He–Cd laser with an output power of 30 mW, 50-mm collection optics, a 0.5-m scanning grating monochromator and an air-cooled GaAs photo multiplier tube (PMT). The emitting light from the sample was focused into the entrance slit of a monochromator that had a spectral grating of 1200 groves/mm and then it was amplified by a PMT. A long-pass filter was inserted after the sample to block any scattered laser light. The cut-off wavelength of the filter at the UV side was about 340 nm.

For PLE measurements, a 1000 W Xe lamp was used to generate white light. The white light passed through a 0.15-m single grating scanning monochromator into a sample chamber. The 2 mm × 3 mm beam size of scanning light was detected by a Si detector before illuminating the sample and then the excitation spectrum was dispersed by a 0.5-m single grating monochromator. The spectrum was collected by an air-cooled GaAs PMT. X-ray diffraction measurements were performed at room temperature. Raman spectra were measured at room temperature in backscattering geometry with a microscope using a diode pumped semiconductor laser with $\lambda = 532$ nm, as the excitation source.

3. Results and discussions

Fig. 1 shows XRD patterns of SnO_2 along with Eu_2O_3 addition. The diffraction patterns of SnO_2 correspond to the all the reported peaks in JCPDS (21-1250). No characteristic peaks of impurities are observed from sintered SnO_2. The calculated lattice constants and unit cell volume of sintered tetragonal SnO_2 are $a = 4.738$, $c = 3.187$ Å, and 71.55 Å^3, respectively, and are agreed to the values obtained from JCPDS. All the peaks pertaining to Eu_2O_3 are depicted as closed circles. Reduction of diffraction peak intensities and a slight diffraction angle shift to high angles are observed, and result in a small contraction of lattice constants ($a = 4.732$, $c = 3.183$ Å) and a decrease of unit cell volume (71.27 Å^3) with the addition of Eu_2O_3. Further, the diffraction peaks associated with Eu_2O_3 become strong with the increase of Eu_2O_3. It is further noticed

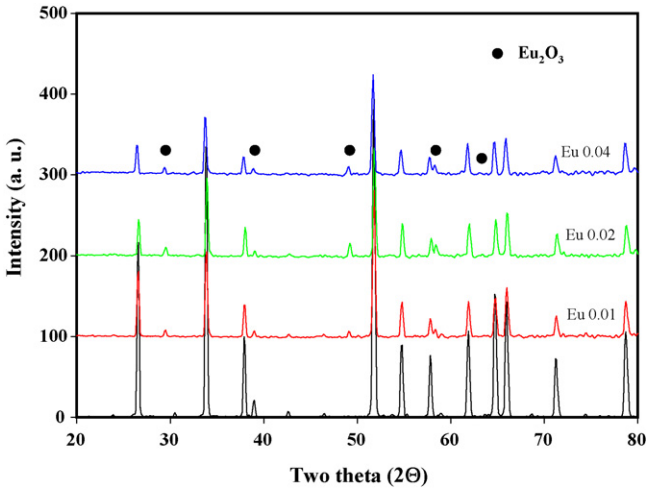

Fig. 1. X-ray diffraction patterns of SnO_2 with Eu_2O_3 addition. The addition of Eu_2O_3 is indicated.

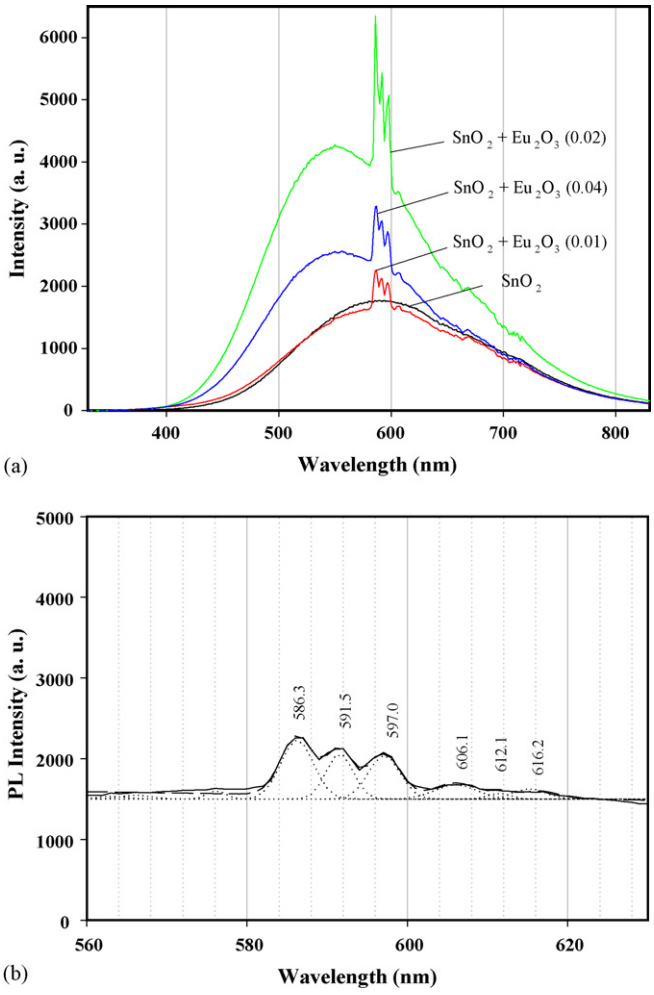

Fig. 2. (a) Room temperature PL spectra of bulk SnO_2 and SnO_2 with Eu_2O_3. (b) The deconvoluted peaks of the luminescence. The fitted spectra are depicted as dotted lines. Gaussian curve fitting is assumed in the figure.

that even 0.01 mol addition of Eu_2O_3 on SnO_2 yield the diffraction peaks of Eu_2O_3. The diffraction peaks associated with Eu_2O_3 become strong with the further addition of Eu_2O_3.

Room temperature PL spectra of the bulk SnO_2 as well as the addition of Eu_2O_3 are depicted in Fig. 2 (a). The bulk SnO_2 shows a broad luminescence covering the whole visible spectral range with PL peak max at 590 nm. There exist some interesting results with the addition of Eu_2O_3. Specifically, a small addition of Eu_2O_3 (0.01 mol) shows an almost identical PL peak compared to the bulk SnO_2. Further addition of Eu_2O_3 yields a slight blue shift of the PL peak max position to 550 nm of host material. The PL intensity reaches maximum (about two times increase) with the 0.02 mol addition of Eu_2O_3 and then decrease with further addition of Eu_2O_3. The most distinct change with the Eu addition is the evolving of rare-earth related luminescence bands near 590 nm. In order to see clearly on the Eu-related luminescence emission, the narrow region of spectra are depicted in Fig. 2 (b), along with deconvoluted peaks assuming a Gaussian peak. Emission bands with a dominant peak at 586 and 606 nm are detected. The emission spectrum of Eu^{3+} is usually sharp and discrete in nature. These peaks correspond to the $^5D_0$–$^7F_1$ and $^5D_0$–$^7F_2$ transitions for Eu^{3+},

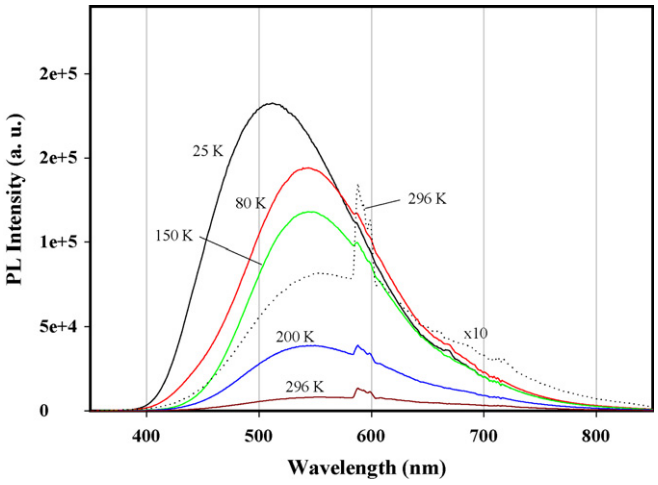

Fig. 3. Low temperature PL spectra of SnO_2 with Eu_2O_3 addition. Measurement temperatures are indicated.

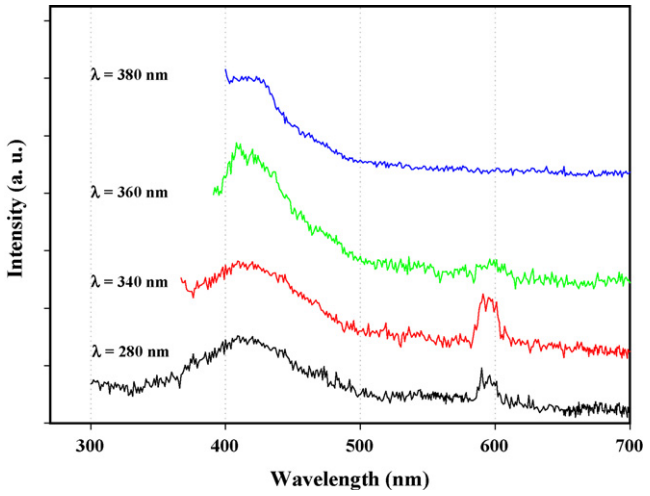

Fig. 4. Photoluminescence emission spectra with different excitation wavelength. Excitation wavelengths are indicated.

respectively [13]. The $^5D_0$–$^7F_1$ emission lines consist of three components at 586, 592, and 597 nm, respectively. The $^5D_0$–$^7F_2$ transition lines display weak peaks at 606, 612, and 616 nm, respectively. The $^5D_0$–$^7F_1$ transition exhibits more intensity than that of $^5D_0$–$^7F_2$ transitions due to localized energy transfers. It is known that the $^5D_0$–$^7F_1$ and $^5D_0$–$^7F_2$ transitions corresponds to orange-red and red color. The red emission ($^5D_0$–$^7F_2$) is due to electric dipole transition, while orange emission ($^5D_0$–$^7F_1$) corresponds to the magnetic dipole transition. The relative intensity ratio between the red emission ($^5D_0$–$^7F_2$) and orange emission (R/O value) is in the range between 0.6 and 0.8. The emission peak intensity ($^5D_0$–$^7F_1$) increases with the addition of Eu_2O_3 up to 0.02 mol, then the further addition of Eu results in a decrease of intensity of $^5D_0$–$^7F_1$ transition. Whereas, the PL peak positions of $^5D_0$–$^7F_1$ and $^5D_0$–$^7F_2$ transitions remain unaltered with the addition of Eu_2O_3. The low temperature PL spectra of Eu-added SnO_2 are depicted in Fig. 3. The blue shift of luminescence peak associated with host material is detected with decrease of temperature. However, the PL peak position and shape of $^5D_0$–$^7F_1$ are quite similar at low temperature with decreased intensities.

The room temperature emission spectra of SnO_2 with 0.02 mol Eu_2O_3 addition are shown in Fig. 4. Excitation energy higher than 3.6 eV clearly exhibits $^5D_0$–$^7F_1$ transitions. In contrast to this, excitation energy below 3.6 eV displays no $^5D_0$–$^7F_1$ transition corresponding to the Eu^{3+}. The reported band gap of SnO_2 is 3.6 eV at room temperature. Thus, the excitation energy higher than 3.6 eV would cause excitation from valence band to conduction band transition and some of the excited photons relax to the defect states, which act as radiative centers, and other electrons are transferred to the Eu^{3+}, and result in the characteristic emission pertaining to $^5D_0$–$^7F_1$ transitions. However, ZnO with the addition of rare-earth material by solid-state reaction only yields green emission from ZnO, which present as electronic defects in the forbidden band. The PL spectra exhibit typical emissions of ZnO with traces of the rare-earth. However, no emission of rare-earth is detected when the excitation wavelength is smaller than 385 nm [14,15]. Thus, no energy transfer can be inferred from ZnO with rare-earth addition. It is quite interesting to note that one could observe the energy transfer between host SnO_2 lattice and rare-earth ions, even though there might be small amount of europium ions into the SnO_2 lattice by solid state sintering (see Fig. 1. Even 0.01 mol addition of Eu_2O_3 on SnO_2 still yields Eu_2O_3 diffraction peaks).

The photoluminescence excitation (PLE) spectrum of SnO_2 with 0.02 mol addition of Eu_2O_3 reveals one broad band at 330 nm corresponding to the transition from valence band to conduction band of SnO_2 and three weak peaks at 430, 480, and 520 nm, as shown in Fig. 5. (All the PLE spectra of Eu_2O_3 addition yield similar results.)

Fig. 6 depicts the room temperature Raman spectra of the bulk SnO_2 along with the addition of Eu_2O_3 on SnO_2. Rutile SnO_2 belongs to the space group D_{4h} and four first order Raman active modes are B_{1g}, E_g, A_{1g}, and B_{2g} [16]. The bulk SnO_2 (Fig. 6) displays the distinct Raman peaks at 475, 634, and 781 cm^{-1}, corresponding to the E_g, A_{1g}, and B_{2g}, respectively

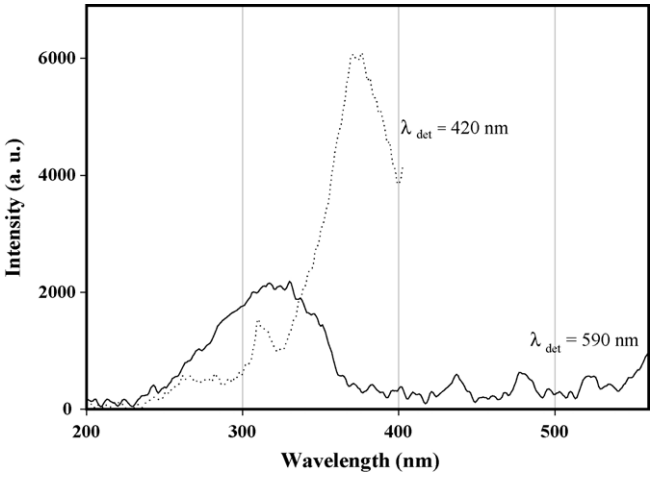

Fig. 5. Photoluminescence excitation spectra obtained for SnO_2 with Eu_2O_3 addition. Detection wavelengths are indicated.

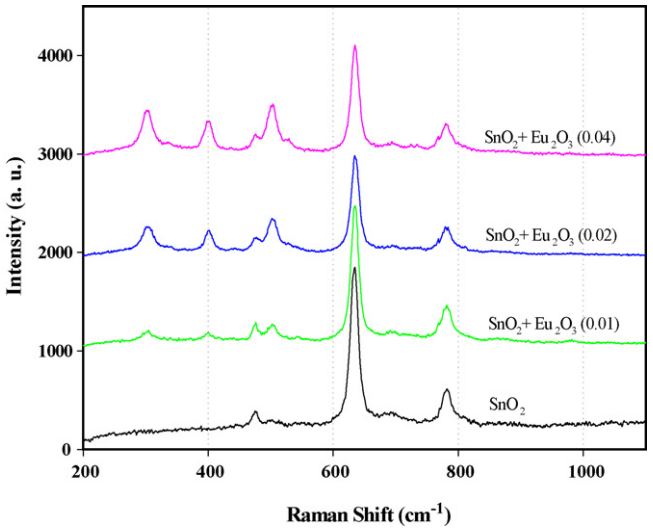

Fig. 6. Room temperature Raman spectra of bulk SnO_2, and SnO_2 with Eu_2O_3.

[16]. Two weak Raman peaks at 501 and 692 cm^{-1} are also detected. These two peaks can be assigned to the A_{2u} and $E_{u(2)}$ mode, respectively [17]. The addition of Eu_2O_3 yields some interesting results of Raman spectra. Specifically, the major vibrational peak position corresponding to SnO_2 (E_g, A_{1g}, and B_{2g}) remains unaltered with the addition of Eu_2O_3. However, the intensities of these vibrational modes decrease with the increase of Eu addition. Furthermore, two vibrational modes (A_{2u} and $E_{u(2)}$) at 501 and 692 cm^{-1} are shifted to 503 and 694 cm^{-1} at 0.04 mol addition of Eu_2O_3. Raman spectra of Eu-added SnO_2 exhibit three additional well resolved novel peaks at 304, 400, and 502 cm^{-1} along with SnO_2 vibrational modes. The more Eu_2O_3 are added on SnO_2, the stronger the intensities of these newly detected vibrational modes become. The reported Raman peaks of Eu_2O_3 are 315, 412, 579, and 610 cm^{-1} [18]. Thus, the observed vibrational modes are not related to Eu_2O_3. It is usually detected that the disorder induces the spectral changes of bulk crystal spectra. It can be further seen that the intensity of these new bands are increase with a decrease of the major vibration mode corresponding to SnO_2, indicating the increase of disorder. This result is consistent with the reduced diffraction peak intensities of XRD analysis in Fig. 2.

4. Conclusions

In this work, the luminescence properties of Eu-added SnO_2 are carried out to find out the feasibility of SnO_2-based phosphor. The Eu-added SnO_2 displays efficient emission lines at 586, 592, and 597 nm, which is associated with the $^5D_0$–$^7F_1$ transitions, along with a broad emission in the 580 nm. It is concluded that the excitation wavelength above 340 nm (3.6 eV) results in energy transfer between host SnO_2 lattice and Eu.

References

[1] D.S. Kumar, P.R. Carbarrocas, J.M. Siefert, In situ investigation of the optoelectronic properties of transparent conducting oxide/amorphous silicon interfaces, Appl. Phys. Lett. 54 (1989) 2088–2090.
[2] A. Lousa, S. Gimeno, J. Martí, Preparation conditions of transparent and conductive SnO2 thin films by reactive evaporation, Vacuum 45 (1994) 1143–1145.
[3] A. Tsunashima, H. Yoshimizu, K. Kodaira, S. Shimada, T. Matsushita, Preparation and properties of antimony-doped SnO_2 films by thermal decomposition of tin 2-ethylhexanoate, J. Mater. Sci. 21 (1986) 2731–2734.
[4] S. Ferrere, A. Zaban, B.A. Gregg, Dye sensitization of nanocrystalline tin oxide by perylene derivatives, J. Phys. Chem. B 101 (1997) 4490–4493.
[5] Y. Tachibana, K. Hara, S. Takano, K. Sayama, H. Arkawa, Investigations on anodic photocurrent loss processes on dye sensitized solar cells: comparison between nanocrystalline SnO_2 and TiO_2 films, Chem. Phys. Lett. 364 (2002) 297–302.
[6] D. Wang, S. Wen, J. Chen, S. Zhang, F. Li, Microstructure of SnO_2, Phys. Rev. B49 (1994) 14282–14285.
[7] Sung-Sik Chang, Dong Kee Park, Novel Sn powder preparation by spark processing and luminescence properties, Mater. Sci. Eng. B 95 (2002) 55–60.
[8] F. Gu, S.F. Wang, M.K. Lu, X.F. Cheng, S.W. Liu, G.J. Zhou, D. Xu, D.R. Yuan, Luminescence SnO_2 thin films prepared by spin-coating method, J. Cryst. Growth 262 (2004) 182–185.
[9] J. Jeong, S.-P. Choi, C.I. Chang, D.C. Shin, J.S. Park, B.-T. Lee, Y.-J. Park, H.-J. Song, Photoluminescence properties of SnO_2 thin films grown by CVD, Solid State Commun. 127 (2003) 595–597.
[10] J. Gouteron, D. Michel, A.M. Lejus, J. Zarembowitch, Raman spectra of lanthanide sesquioxide single crystals: correlation between A and B-type structures, J. Solid State Chem. 38 (1981) 288–296.
[11] H. Nakane, A. Hoya, S. Kuriki, G. Matsumoto, Dielectric properties of europium oxide films, Thin Solid Films 59 (1979) 291–293.
[12] M.K. Jayaraj, C.P.G. Vallabhan, Dielectric and optical properties of europium oxide films, Thin Solid Films 177 (1989) 59.
[13] U. Rambadu, N.R. Munirathnam, T.L. Prakash, S. Suddhudu, Emission spectra of $LnPO_4$:RE^{3+} (Ln = La, Gd; RE = Eu, Tb, and Ce) powder phosphors, Mater. Chem. Phys. 78 (2002) 160–169.
[14] D. Kouyate, J.-C. Ronfard-Haret, J. Kossanyi, Photo- and electro-luminescence of rare earth-doped semiconducting zinc oxide electrodes: Emission from both the dopant and the support, J. Lumin. 50 (1991) 205.
[15] S.A.M. Lima, F.A. Sigoli, M.R. Davolos, M. Jafelicci Jr., Europium(III)-containing zinc oxide from Pechini method, J. Alloys Compd. 344 (2002) 280–284.
[16] S.P.S. Porto, P.A. Fleury, T.C. Damen, Raman spectra of TiO_2, MgF_2, ZnF_2, and MnF_2, Phys. Rev. 154 (1967) 522–526.
[17] J.X. Wang, D.F. Liu, X.Q. Yan, H.J. Yuan, L.J. Ci, Z.P. Zhou, Y. Gao, L. Song, L.F. Liu, W.Y. Zhou, G. Wang, S.S. Xie, Growth of SnO_2 nanowires with uniform branched structures, Solid State Commun. 130 (2004) 89–94.
[18] S. Wang, W. Wang, Y. Qian, Preparation and characterization of Eu_2O_3 nanometer thin films by pulse ultrasonic spray pyrolysis method, Mater. Res. Bull. 35 (2000) 2057–2062.